Supplementary Information (SI) for Reaction Chemistry & Engineering.
This journal is © The Royal Society of Chemistry 2025

Supplementary Information

Uncertainty Quantification analysis of electrochemical reduction of CO2

Hariharan R K and Himanshu Goyal*

Department of Chemical Engineering, Indian Institute of Technology Madras, Chennai, Tamil Nadu 600036, India

* E-mail: goyal@iitm.ac.in

S1 Grid Independence Study

A grid independent study is performed for the developed 1D model. To ensure the grid independence, the concentration of CO_2 at the electrode surface and the total interface current density is used as targets. In COMSOL, five types of physics-based meshes are used: Extremely fine, Extra fine, Finer, Normal, and Coarser. Figure S1 and Figure S3 show that the concentrations at the electrode surface for a voltage range (0 to -2 V vs Ag/AgCl) are almost the same. We see both the profiles across the voltage -2 to 0 V vs Ag/AgCl exhibit grid independence.

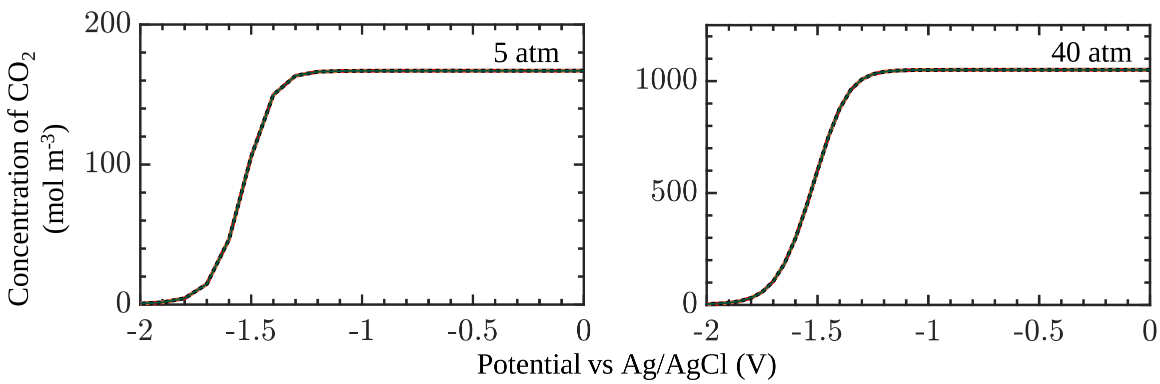

Figure S1: Concentration vs voltage for different grid resolutions used to solve the 1D model in COMSOL at 5 atm (left) and 40 atm (right). Five mesh types are used to confirm the grid independence. 1. Extremely fine (mesh elements: 100); 2. Extra fine (mesh elements: 50); 3, Finer (mesh elements: 27); 4. Normal (15); 5. Coarser (8).

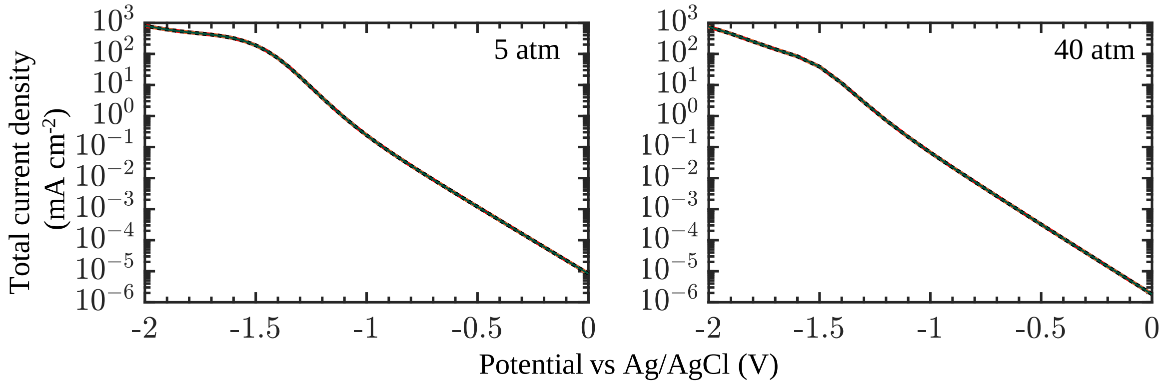

Figure S2: Current density vs voltage for different grid resolutions used to solve the 1D model in COMSOL at 5 atm (left) and 40 atm (right). Five mesh types are used to confirm the grid independence.

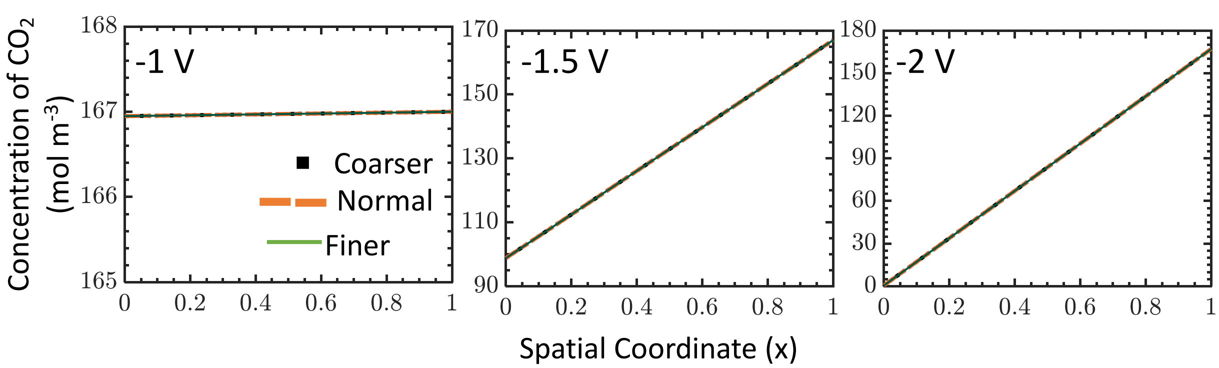

Figure S3: CO2 concentration vs spatial coordinate for different grid resolutions used to solve the 1D model in COMSOL at 5 atm. The results are shown for Finer (mesh elements: 27), Normal (mesh elements: 15), and Coarser (mesh elements: 8).

S2 Identification of regimes for Sensitivity Analysis

The sensitivity analysis is performed for sixteen parameters to identify the parameters that impact the model predictions the most. The sensitivity analysis is performed in kinetic limiting, mixed, and mass transfer limiting regimes. The regimes can be identified from the concentration of CO_2 at the cathode surface as shown in Figure S4.

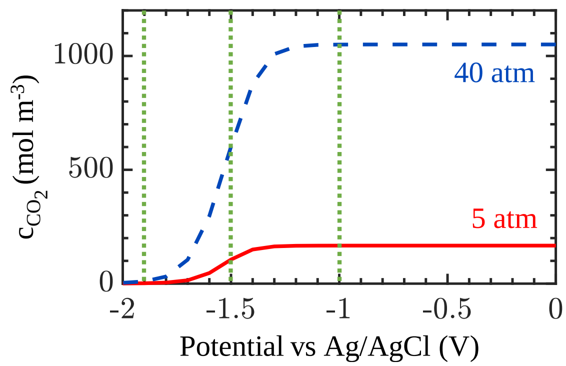

Figure S4: Concentration of CO_2 at the cathode surface at 5 atm (solid red line) and 40 atm (dashed blue line). Dotted green lines indicate the voltages used for the sensitivity analysis.

S3 Parameters for calculating Sechenov's constant

Table S1: Parameters used for the calculation of Sechenov's constant

Parameter	**Value**
$h^0_{CO_2}$	-0.0172
$h^T_{CO_2}$	-0.00034
$h_{HCO_3^-}$	0.0967
$h_{CO_3^{2-}}$	0.1423
h_{K^+}	0.0922
h_{OH^-}	0.0839

S4 List of studies used for uncertainty characterization

Table S2: Sample names and their abbreviations used in section 4.2.2 in main text

Study	Sample Name	Abbreviation
SSP - 1[1]	Indium wire	In-Wr
SSP - 2[2]	Commercial Indium Foil	In-f
SSP - 3[3]	Electrodeposited Indium	RE-In
LSV - 1[4]	Commercial Indium foil	In-f
	Electrodeposited dendritic In	DF-In
	Regular In electrodeposited	RE-In
	Cl^- ion assisted dendritic In	CADF-In
LSV - 2[5]	Conventional wet-chemistry method In nanoparticle	W-In
	Laser activated Indium	L-In
	Commercial Indium Powder	C-In
LSV - 3[6]	Indium Deposit	In-D
	Atomically Dispersed Indium	In-N-C

Table S3: Preparation methods for different samples in various studies

Study	**Sample**	**Preparation method**
SSP-1	In wire	Purchased from Kanto Chemical Co. Ltd, and polished by soft paper and an abrasive
SSP-2	Commercial In foil	Purchased from Alfa Aesar and further cleaned with acetone, water, 2 M HCl for 5 mins and Milli-Q water
SSP-3	Electrodeposited In	40 nm Au film sputtered on Si Wafers, In was electrodeposited on this using 50 mM $In_2(SO_4)_2$, 0.5 M H_2SO_4 and 0.5 M NaCl. Depositions were performed at -2.05 V
LSV-1	Commercial In foil	Purchased from Alfa Aesar and mechanically polished by 400 grit sandpaper
	Electrodeposited dendritic In	Prepared using Cu and graphite plate as working and counter electrode respectively, the electrolyte used was 0.01 M of $InCl_3$ in 0.5 M H_2SO_4. The deposition is carried at a current density of 2 A cm^{-2}
	Regular In electrodeposited	Prepared using Cu and graphite plate as working and counter electrode respectively, the electrolyte used was 0.05 M of $InCl_3$ in 0.5 M H_2SO_4. The deposition is carried at a current density of 2 A cm^{-2}
	Cl^- ion assisted dendritic In	Prepared using Cu and graphite plate as working and counter electrode respectively, the electrolyte used was 0.05 M of $InCl_3$ in 0.5 M NH_4Cl. The deposition is carried at a current density of 2 A cm^{-2}
LSV-2	Conventional wet-chemistry method In nanoparticle	Prepared by heating mixture of $In(ac)_3$, oleylamine and $NaBH_4$ at 120°C for 2h followed by cooling and centrifuging
	Laser activated Indium	Laser In was created by converting $InCl_3$ 10.6 μm, 60 W, CO_2 laser marker
	Commercial In powder	Purchased from Macklin
LSV-3	Indium Deposit	Prepared by using carbon cloth as a substrate in 40 mg of $In_2(SO_4)_2$ in 50 mL of ultra pure water at potential of -0.1 V vs SCE
	Atomically dispersed In	Prepared on In doped Zn 2-methylimidazolate framework at 900°C in N_2 atmosphere

S5 List of fitted kinetic parameters from the literature used for UQ

The following kinetic parameters were obtained by fitting the polarization data using least squares. The linear regression is performed for the same data set multiple times by changing the number of points (DPs) considered in the Tafel region. These fitted kinetic parameters were used to quantify the uncertainties in section 4.2.2 of the main text.

Table S4: Formate kinetic parameters

S.No	**i_0**	α_c	**R^2**	**DPs**	**Study**	**Sample**
1	4.739E-07	0.456	0.994	4	SSP-1	In-Wr
2	2.433E-07	0.478	1.000	3	SSP-2	In-Wr
3	7.396E-06	0.264	0.970	8	SSP-2	In-f
4	2.260E-06	0.292	0.984	7	SSP-2	In-f
5	1.055E-06	0.311	0.989	6	SSP-2	In-f
6	8.270E-07	0.317	0.982	5	SSP-2	In-f
7	1.099E-06	0.310	0.964	4	SSP-2	In-f
8	1.461E-05	0.244	0.969	3	SSP-2	In-f
9	4.182E-05	0.199	0.857	4	SSP-3	RE-In
10	4.486E-06	0.256	0.976	3	SSP-3	RE-In
11	3.333E-04	0.284	0.912	6	LSV-1	In-f
12	8.478E-05	0.351	0.959	5	LSV-1	In-f
13	3.195E-05	0.402	0.983	4	LSV-1	In-f
14	1.135E-05	0.458	0.999	3	LSV-1	In-f
15	1.162E-02	0.209	0.814	7	LSV-1	DF-In
16	5.197E-03	0.257	0.884	6	LSV-1	DF-In
17	2.732E-03	0.298	0.924	5	LSV-1	DF-In

Continued on next page

Table S4 – *Continued from previous page*

S.No	i_0	α_c	R^2	DPs	Study	Sample
18	1.233E-03	0.351	0.958	4	LSV-1	DF-In
19	4.504E-04	0.423	0.997	3	LSV-1	DF-In
20	1.102E-03	0.256	0.854	6	LSV-1	RE-In
21	2.812E-04	0.325	0.940	5	LSV-1	RE-In
22	1.027E-04	0.378	0.963	4	LSV-1	RE-In
23	2.858E-05	0.449	0.995	3	LSV-1	RE-In
24	1.375E-02	0.219	0.802	7	LSV-1	CADF-In
25	5.743E-03	0.270	0.845	6	LSV-1	CADF-In
26	2.783E-03	0.317	0.877	5	LSV-1	CADF-In
27	1.090E-03	0.380	0.898	4	LSV-1	CADF-In
28	2.849E-04	0.478	0.942	3	LSV-1	CADF-In
29	1.956E-04	0.220	0.974	7	LSV-2	W-In
30	1.229E-04	0.234	0.972	6	LSV-2	W-In
31	1.102E-04	0.237	0.952	5	LSV-2	W-In
32	1.427E-04	0.229	0.905	4	LSV-2	W-In
33	4.606E-04	0.191	0.796	3	LSV-2	W-In
34	4.091E-05	0.260	0.994	5	LSV-2	W-In
35	1.433E-05	0.290	0.999	3	LSV-2	W-In
36	3.174E-02	0.153	0.960	7	LSV-2	L-In
37	2.358E-02	0.168	0.977	6	LSV-2	L-In
38	1.402E-02	0.185	0.991	5	LSV-2	L-In
39	1.402E-02	0.197	0.993	4	LSV-2	L-In
40	1.920E-02	0.178	0.998	3	LSV-2	L-In
41	8.568E-04	0.168	0.973	7	LSV-2	C-In

Continued on next page

Table S4 – *Continued from previous page*

S.No	i_0	α_c	R^2	DPs	Study	Sample
42	7.889E-04	0.171	0.957	6	LSV-2	C-In
43	1.106E-03	0.160	0.931	5	LSV-2	C-In
44	1.508E-03	0.151	0.869	4	LSV-2	C-In
45	4.850E-04	0.189	0.802	3	LSV-2	C-In
46	1.472E-04	0.244	0.843	4	LSV-3	In-D
47	1.213E-05	0.316	0.966	3	LSV-3	In-D
48	2.067E-03	0.200	0.865	5	LSV-3	In-N-C
49	5.287E-04	0.243	0.900	4	LSV-3	In-N-C
50	7.002E-05	0.307	0.991	3	LSV-3	In-N-C

Table S5: Carbon Monoxide kinetic parameters

S.No	i_0	α_c	R^2	DPs	Study	Sample
1	3.870E-04	0.233	0.974	4	SSP-1	In-Wr
2	2.328E-04	0.253	0.999	3	SSP-1	In-Wr
3	2.615E-04	0.154	0.859	8	SSP-2	In-f
4	9.633E-05	0.181	0.928	7	SSP-2	In-f
5	5.220E-05	0.200	0.922	6	SSP-2	In-f
6	1.940E-05	0.225	0.921	5	SSP-2	In-f
7	4.330E-06	0.268	0.992	4	SSP-2	In-f
8	3.775E-05	0.244	0.985	3	SSP-2	In-f
9	1.110E-03	0.098	0.999	3	SSP-3	RE-In
10	4.765E-03	0.068	0.910	3	LSV-1	In-f
11	6.307E-02	0.054	0.820	4	LSV-1	DF-In
12	3.649E-02	0.071	0.824	3	LSV-1	DF-In

Continued on next page

Table S5 – *Continued from previous page*

S.No	i_0	α_c	R^2	DPs	Study	Sample
13	6.033E-03	0.092	0.956	4	LSV-1	RE-In
14	3.450E-03	0.109	0.964	3	LSV-1	RE-In
15	1.060E-02	0.093	0.864	4	LSV-1	CADF-In
16	4.678E-03	0.119	0.975	3	LSV-1	CADF-In
17	5.414E-03	0.111	0.787	5	LSV-2	W-In
18	6.330E-03	0.116	0.927	3	LSV-2	W-In
19	2.261E-02	0.094	0.850	6	LSV-2	L-In
20	1.498E-02	0.111	0.878	5	LSV-2	L-In
21	8.601E-03	0.134	0.913	4	LSV-2	L-In
22	4.035E-03	0.168	0.962	3	LSV-2	L-In
23	6.739E-03	0.110	0.985	4	LSV-2	C-In
24	7.610E-03	0.106	0.966	3	LSV-2	C-In
25	2.594E-03	0.136	0.932	5	LSV-3	In-D
26	1.386E-03	0.155	0.912	4	LSV-3	In-D
27	9.544E-04	0.167	0.788	3	LSV-3	In-D
28	2.672E-01	0.032	0.992	6	LSV-3	In-N-C
29	2.535E-01	0.033	0.994	5	LSV-3	In-N-C
30	2.393E-01	0.035	0.996	4	LSV-3	In-N-C
31	2.244E-01	0.037	0.998	3	LSV-3	In-N-C

Table S6: Hydrogen kinetic parameters

S.No	i_0	α_c	R^2	DPs	Study	Sample
1	7.050E-05	0.275	0.993	6	SSP-1	In-Wr
2	4.197E-05	0.290	0.987	5	SSP-1	In-Wr

Continued on next page

Table S6 – *Continued from previous page*

S.No	i_0	α_c	R^2	DPs	Study	Sample
3	2.674E-05	0.306	0.988	4	SSP-1	In-Wr
4	6.854E-05	0.274	0.967	3	SSP-1	In-Wr
5	3.011E-03	0.116	0.878	8	SSP-2	In-f
6	1.326E-03	0.135	0.907	7	SSP-2	In-f
7	6.558E-04	0.153	0.938	6	SSP-2	In-f
8	5.891E-04	0.155	0.892	5	SSP-2	In-f
9	5.336E-04	0.158	0.785	4	SSP-2	In-f
10	3.785E-03	0.112	0.965	4	SSP-3	RE-In
11	1.666E-03	0.132	0.988	3	SSP-3	RE-In
12	2.864E-03	0.119	0.970	4	LSV-1	In-f
13	3.943E-03	0.111	0.936	3	LSV-1	In-f
14	3.165E-02	0.083	0.998	4	LSV-1	DF-In
15	3.394E-02	0.081	0.995	3	LSV-1	DF-In
16	1.556E-03	0.145	0.996	4	LSV-1	RE-In
17	1.082E-03	0.154	0.999	3	LSV-1	RE-In
18	1.168E-02	0.106	0.995	4	LSV-1	CADF-In
19	8.496E-03	0.114	0.999	3	LSV-1	CADF-In
20	3.231E-03	0.149	0.992	5	LSV-2	W-In
21	2.418E-03	0.160	0.996	4	LSV-2	W-In
22	2.144E-03	0.165	0.992	3	LSV-2	W-In
23	8.814E-03	0.118	0.886	5	LSV-2	L-In
24	1.270E-02	0.107	0.787	4	LSV-2	L-In
25	4.544E-03	0.147	0.994	4	LSV-2	C-In
26	5.435E-03	0.141	0.988	3	LSV-2	C-In

Continued on next page

Table S6 – *Continued from previous page*

S.No	$\mathbf{i}_0$	α_c	$\mathbf{R^2}$	**DPs**	**Study**	**Sample**
27	2.170E-01	0.033	0.970	5	LSV-3	In-D
28	2.030E-01	0.035	0.965	4	LSV-3	In-D
29	1.883E-01	0.037	0.999	3	LSV-3	In-D
30	1.165E-04	0.200	0.990	4	LSV-3	In-N-C
31	8.293E-05	0.208	0.979	3	LSV-3	In-N-C

S6 Apparent relation between i_0 and α_c

The uncertainty in the model parameters is characterized by the probability distribution function, and it is sampled for uncertainty propagation. For estimating the uncertainty due to manual truncation of polarization data α_c is characterized by uniform distribution. For sampling i_0, we construct an apparent relation between α_c and i_0, and then use the sampled α_c to get i_0. The apparent distribution for Case 1 in section 4.2.1 and Case 2 in section 4.2.2 in the main text are given in figure S5 and S6, respectively. This approach ensures that the combination of the sampled values is physically and computationally feasible. Also, it helps us to include the inverse proportionality between α_c and i_0.

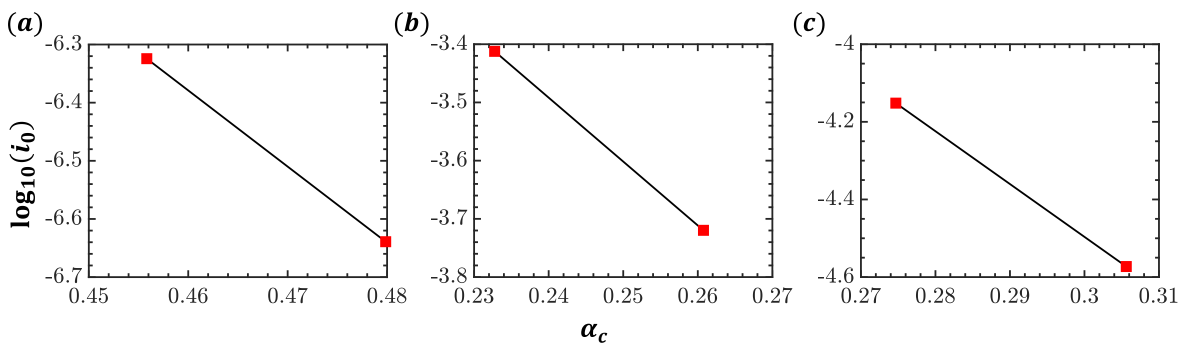

Figure S5: Apparent relation between i_0 and α_c for a) CO_2RR b) COER c) HER reaction corresponding to Case 1 in section 4.2.1. This apparent reaction corresponds to maximum i_0 and minimum α_c and minimum i_0 and maximum α_c obtained from fitting polarization data. The apparent relations for CO_2RR, COER and HER are $\log_{10}(i_0) = -13.098\alpha_c - 0.354$, $\log_{10}(i_0) = -10.978\alpha_c - 0.857$ and $\log_{10}(i_0) = -13.391\alpha_c - 0.480$, respectively

.

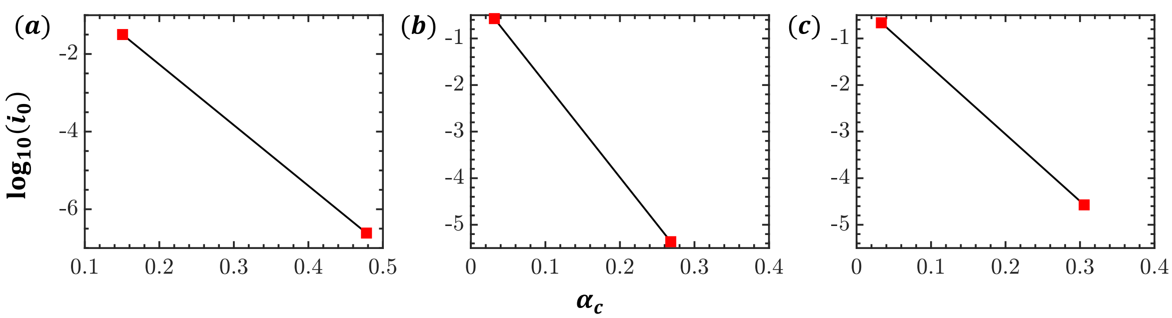

Figure S6: Apparent relation between i_0 and α_c for a) CO_2RR b) COER c) HER reaction corresponding to Case 2 in section 4.2.2. This apparent reaction corresponds to maximum i_0 and minimum α_c and minimum i_0 and maximum α_c obtained from fitting polarization data. The apparent relations for CO_2RR, COER and HER are $\log_{10}(i_0) = -15.633\alpha_c + 0.858$, $\log_{10}(i_0) = -20.243\alpha_c + 0.0657$ and $\log_{10}(i_0) = -14.354\alpha_c - 0.186$, respectively

.

S7 Effect of number of sampling on the uncertainty results

Table S7: Mean of the partial current density (in mA) computed across all voltages for the electrochemical reactions obtained from 4000, 5000, and 6000 samples.

Sample size $\mathcal{N}$	CO2RR	COER	HER
4000	15.8039	0.1162	10.3944
5000	15.8105	0.1164	10.4036
6000	15.8064	0.1163	10.3719

Table S8: Mean 95% confidence interval width obtained from 4000, 5000, and 6000 samples.

Sample size $\mathcal{N}$	CO2RR	COER	HER
4000	9.3667	0.3965	64.5902
5000	9.3544	0.3960	64.5901
6000	9.3343	0.3964	64.2963

S8 List of the uncertain parameters used in the uncertainty propagation along with their properties.

Table S9: List of uncertain parameters, their distributions, and the corresponding sensitive outputs/targets.

Uncertain parameter	**Choice of uncertainty distribution in section 5.2.1**	**Choice of uncertainty distribution in section 5.2.1**	**Sensitive target parameters**
Exchange current density CO_2RR	Sampled from relation between i_0 and α_c	Sampled from relation between i_0 and α_c	Partial current density of CO_2RR
Exchange current density COER	Sampled from relation between i_0 and α_c	Sampled from relation between i_0 and α_c	Partial current density of COER
Exchange current density HER	Sampled from relation between i_0 and α_c	Sampled from relation between i_0 and α_c	Partial current density of COER and HER
Transfer coefficient CO_2RR	Uniform distribution	KDE-based distribution	Partial current density of CO_2RR and COER
Transfer coefficient COER	Uniform distribution	KDE-based distribution	Partial current density of CO_2RR and COER
Transfer coefficient HER	Uniform distribution	KDE-based distribution	Partial current density of CO_2RR, COER and HER

S9 Uncertainty quantification of model predictions at 40 atm

The procedure for uncertainty quantification of 40 atm cases is similar to that of 5 atm. The quantified predictions from the uncertainty propagation are compared with experimental data[1] at 40 atm from the literature. Figure S7 shows the uncertainty due to human bias in manual truncation of the kinetic regime for fitting the Tafel equation to estimate kinetic parameters at 40 atm. Figure S8 shows the uncertainty in the model prediction due to human bias in fitting Tafel data, sample preparation and polarization data source technique (SSP vs LSV). These results are similar to their 5 atm counterparts.

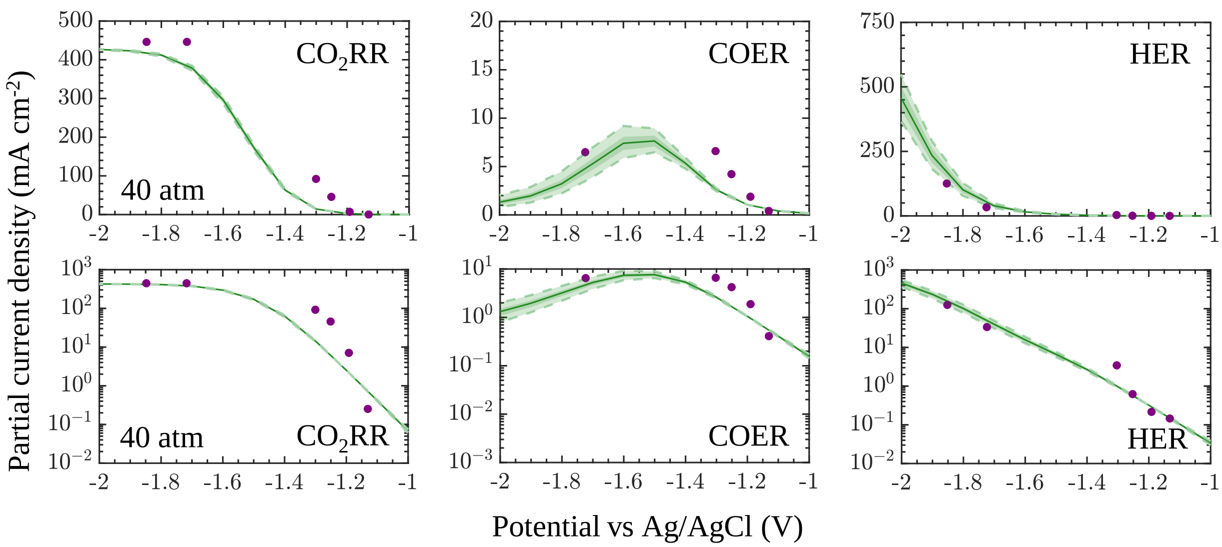

Figure S7: Model predictions with quantified uncertainty and the experimental measurements (symbols) of the partial current density of all three electrochemical reactions at 40 atm. The uncertainty in the kinetic parameters is due to human bias in fitting Tafel data. The green solid line is the mean of the model predictions. The light green region bounds 2.5 percentile and 97.5 percentile of the predictions covering 95% of the area. The dark green region bounds 25 percentile and 75 percentile of the predictions covering 50% of the area.

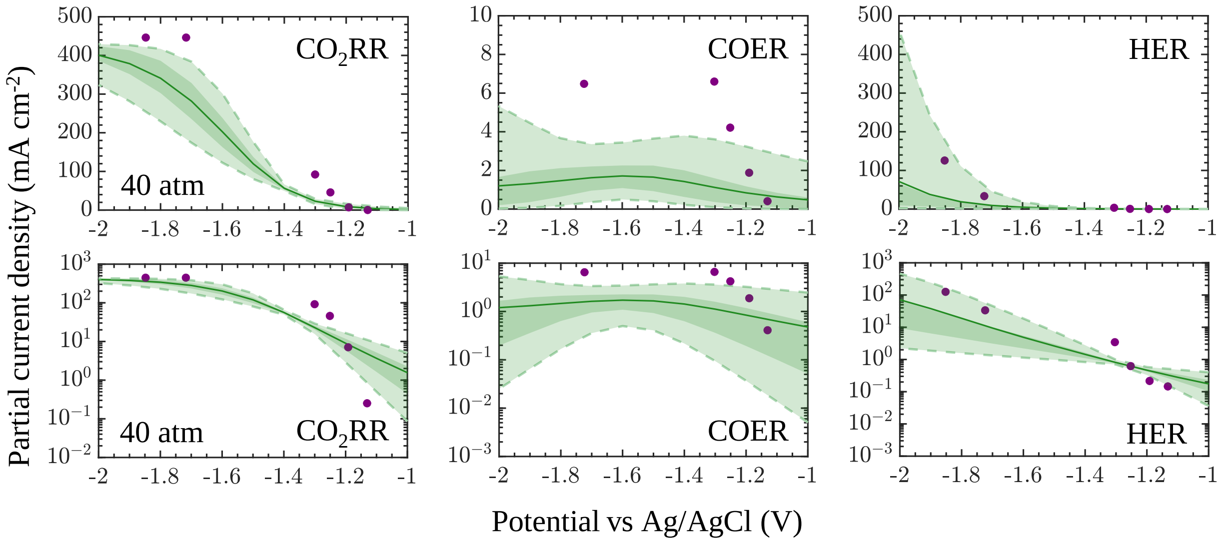

Figure S8: Model predictions with quantified uncertainty and the experimental measurements of the partial current density of all three electrochemical reactions at 40 atm. The uncertainty in the kinetic parameters is due to human bias in fitting Tafel data, polarization data technique (SSP vs LSV), and catalyst preparation. The green solid line is the mean of the model predictions. The light green region bounds 2.5 percentile and 97.5 percentile of the predictions covering 95% of the area. The dark green region bounds 25 percentile and 75 percentile of the predictions covering 50% of the area.

References

(1) Todoroki, M.; Hara, K.; Kudo, A.; Sakata, T. Electrochemical reduction of high pressure CO 2 at Pb, Hg and In electrodes in an aqueous KHCO 3 solution. *Journal of Electroanalytical Chemistry* **1995**, *394*, 199–203.

(2) Luo, W.; Xie, W.; Li, M.; Zhang, J.; Züttel, A. 3D hierarchical porous indium catalyst for highly efficient electroreduction of CO 2. *Journal of Materials Chemistry A* **2019**, *7*, 4505–4515.

(3) Hoffman, Z. B.; Gray, T. S.; Moraveck, K. B.; Gunnoe, T. B.; Zangari, G. Electrochemical Reduction of Carbon Dioxide to Syngas and Formate at Dendritic Copper-Indium Electrocatalysts. *ACS Catalysis* **2017**, *7*, 5381–5390.

(4) Xia, Z.; Freeman, M.; Zhang, D.; Yang, B.; Lei, L.; Li, Z.; Hou, Y. Highly Selective

Electrochemical Conversion of CO2 to HCOOH on Dendritic Indium Foams. *ChemElectroChem* **2018**, *5*, 253–259.

(5) Guo, W. et al. Transient Solid-State Laser Activation of Indium for High-Performance Reduction of CO2 to Formate. *Small* **2022**, *18*.

(6) Lu, P. et al. Atomically Dispersed Indium Sites for Selective CO2Electroreduction to Formic Acid. *ACS Nano* **2021**, *15*, 5671–5678.